

The impact of planetary boundary layer parameterisation scheme over the Yangtze River Delta region, China: Part I – Seasonal and diurnal sensitivity studies

Ansheng Zhu ^{a,b}, Lishu Shi ^{a,b}, Ling Huang ^{a,b}, Ying Gu ^c, Andy Chan ^{d*}, Yangjun Wang ^{a,b}, Li Li ^{a,b*}

^a School of Environmental and Chemical Engineering, Shanghai University, Shanghai 200444, China

^b Key Laboratory of Organic Compound Pollution Control Engineering (MOE), Shanghai University, Shanghai 200444, China

^c School of Air Transportation, Shanghai University of Engineering Science, Shanghai 201620, China

^d Department of Civil Engineering, University of Nottingham Malaysia, Semenyih 43500, Selangor, Malaysia

Correspondence to Li Li (Lily@shu.edu.cn) and Andy Chan (Andy.Chan@nottingham.edu.my)

Abstract: The planetary boundary layer (PBL) is the main region for the exchange of matter, momentum and energy between land and atmosphere. The transport processes in the PBL determine the distribution of temperature, water vapour, wind speed and other physical quantities within the PBL and are very important for the simulation of the physical characteristics of the meteorology. Based on the two non-local closure PBL schemes (YSU, ACM2) and two local closure PBL schemes (MYJ, MYNN) in the Weather Research and Forecasting (WRF) model, seasonal and daily cycles of meteorological variables over the Yangtze River Delta (YRD) region are investigated. It is shown that all the four PBL schemes overestimate 10-m wind speed and 2-m temperature, while underestimate relative humidity. The MYJ scheme produces the largest biases on 10-m wind speed and the smallest biases on humidity, while the ACM2 scheme shows WRF-simulated 2-m temperature and 10-m wind speed are closer to surface meteorological observations in summer. The ACM2 scheme performs well with daytime PBL height, the MYNN scheme performs the lowest mean bias of 0.04 km and the ACM2 scheme shows the highest correlation coefficient of 0.59 compared with observational data. It is found that there is a varying degree of sensitivity of the respective PBL in winter and summer and a best-performing PBL scheme should be chosen to predict various meteorological conditions under different seasons over a complicated region like the YRD.

Keywords: planetary boundary layer scheme; meteorology simulation; seasonal sensitivity; Yangtze River Delta region

Highlights

- WRF model performance with four PBL schemes over the YRD region are evaluated.
- Seasonal and diurnal variations of surface meteorological parameters are presented.
- ACM2 scheme shows good performance during summer while MYJ scheme performs better in winter.

1 Introduction

Through the interaction of surface forcing and turbulent motion, the planetary boundary layer (PBL) leads to mixed exchange between surface water vapour, heat and upper-level momentum, which in turn affects the near-surface meteorological field and diffusion of atmospheric pollutants [Ayotte *et al.*, 1996; Jia and Zhang, 2020; Sullivan *et al.*, 1994]. The structure and variations of the PBL directly reflect changes in surface thermal conditions and are characterised by significant diurnal variations with temperature. Since the turbulent motion of the PBL is generally much smaller than the horizontal grid spacing of existing small- and medium-scale models, sub-grid scale effects need to be considered [Bryan *et al.*, 2003]. The heat and momentum fluxes in the boundary layer are transported by turbulent motions, which are difficult to resolve on the spatial and temporal scales [Penchah *et al.*, 2017] even with general engineering turbulence models, and hence general engineering or application simulations require the introduction of a PBL parameterisation scheme to calculate the physical quantities of heat and momentum in the boundary layer [Draxl *et al.*, 2014; Smith and Thomsen, 2010].

PBL parameterisation scheme mainly describes the vertical transport of atmospheric momentum, heat, water vapour and other physical quantities in the boundary layer [Garratt, 1994]. Uncertainties in the physical parameterisation schemes of models such as cumulus convection, surface processes, and PBL scheme are some of the main causes of errors in the regional climate modeling system [Wang *et al.*, 2014]. Hence the choice and use of parameterisation schemes is of vital importance to the prediction of meteorological fields within the boundary layer, the trajectory study of air pollutant diffusion and the simulation of large-scale weather systems such as typhoons and rainstorms [Bright *et al.*, 2002; Han *et al.*, 2008; Li *et al.*, 2016, Oozeer *et al.*, 2016]. Literally the accuracy of numerical weather prediction depends solely on the choice of a good parameterisation scheme. At present, the parameterisation schemes of numerical models mainly

include simple population parameter method, K-profile method, closed method, original asymmetric convection method and spectral diffusion theory [Hu *et al.*, 2010; Moeng, 1984; Shin and Hong, 2011].

The Weather Research and Forecasting (WRF) [Skamarock *et al.*, 2008], a mesoscale model widely used at present for weather forecasting and research, has many different kinds of boundary layer parameterisation schemes that can be chosen by simply changing the parameterisation options. For the mesoscale model, the resolution of the model in the horizontal and vertical directions is higher than that of the large-scale model, and the boundary layer process can be considered more carefully than the large-scale model. Therefore, some mesoscale phenomena can be simulated in more details. The consideration of the boundary layer is also based on the research results of the boundary layer itself. Due to the importance of boundary layer parameterisation scheme to a successful numerical simulation, many studies examine a large number of sensitivity tests for PBL schemes [Coniglio *et al.*, 2013; Gopalakrishnan *et al.*, 2013; Mohan and Bhati, 2011; Smith and Thomsen, 2010; Yver *et al.*, 2013]. Following the incessant development of models and PBL physics, some comparative studies have been carried out to study the applicability and applications of specific schemes in different regions. However, there is no uniformity in the set of schemes that diagnoses better for each application. Generally, the model performance is under the influence of the season or time of day, the variables considered and the regional characteristics. One cannot determine an optimal set of model configuration in general terms. There are obvious discrepancies among different research conclusions, or the research results depend on individual cases of the study.

PBL schemes are used to describe the vertical fluxes of heat, momentum, moisture due to eddy transport within the whole atmospheric column in the turbulent processes [Banks and Baldasano, 2016]. The number of unknowns of the equations appearing in a turbulent motion equation set is greater than the number of equations sets, making the original closed equation set non-closed, i.e., a set containing an infinite number of equations is needed to fully describe turbulence. To solve this problem, a finite number of equations is used to approximate the unknown quantity, which is known as turbulence modelling [Hariprasad *et al.*, 2014; Holt and Raman, 1988]. One major component of the turbulence processes is whether a local or non-local mixing approach is employed. The local closure schemes obtain the turbulent fluxes using the mean variables and their gradients at each model grid. The non-local closure schemes use multiple vertical levels and profiles of convective boundary layer to determine variables [Cohen *et al.*, 2015]. The sensitivity of different parameterisation schemes is closely related to meteorological and geographical environments. The MM5 model is used by Zhang and Zheng [2004] to simulate surface wind and

temperature in the central part of summer in the United States. Results show that the non-local Blackadar (BLK) scheme performs better in predicting the daily cycle of temperature and surface wind speed compared with other schemes. *Sanjay* [2008] shows that the non-local Troen-Mahrt (TM) scheme coupled to the land surface scheme causes boundary layer transition mixing, resulting in low humidity in the boundary layer under the condition of clear air in northwest India. *Kwun et al.* [2009] simulates the ocean surface wind speed during the typhoon using MM5 (5th generation mesoscale model) and WRF in combination with various parameterization schemes. It is found that the wind speed obtained from the WRF coupled with the Yonsei University (YSU) and Mellor-Yamada-Janjić (MYJ) schemes are most consistent with observations. By quantifying the meteorological elements simulated by four PBL schemes (YSU), asymmetric convection model 2 (ACM2), MYJ, and Bougeault and Lacarrere (BouLac) in the WRF model, *Xie et al.* [2012] shows that the PBL height simulated by the MYJ and BouLac schemes is higher than that by the YSU and ACM2 schemes. It is more conducive to the upward transport of warm and humid airflow and the development of strong convection. *Ooi et al.* [2018] uses the MYJ scheme and studies the momentum and air pollutant transfers during the monsoon climates of Malaysia. *Hu et al.* [2010] evaluates three PBL schemes in the WRF model and found that the non-local YSU scheme and ACM2 scheme simulated strong daytime boundary layer mixing and entrainment, resulting in higher temperatures and lower humidity, while the local MYJ scheme predicted lower temperature and humidity due to weaker mixing and entrainment. At night the mixing of the YSU scheme is stronger than that of the ACM2 and the MYJ schemes, and the predicted temperature is also higher and humidity was lower. *Wang et al.* [2017a] uses the WRF model coupled with four commonly used PBL schemes (ACM2, MYJ, Mellor-Yamada-Nakanishi-Niino Level 2.5 (MYNN2), and YSU) to predict the meteorological elements and boundary layer structure in a typical farmland area of China, and finds that the ACM2 scheme shows good performance on both sunny and cloudy days.

While there are a good number of works studying the sensitivity of the various parameterisation schemes, there is one general commonality in all of these studies: the simulation period is generally very short and is usually concentrated with an episode of meteorological event. The accuracy of the work, hence, cannot or may not be able to be extrapolated to post-event calculations. It is also found that in some cases, while YSU or ACM2 is good for day-time calculations, their performances are generally not the same for night-time or even a different season. Preliminary works [*Chu et al.*, 2019; *García-Díez et al.*, 2013; *Kala et al.*, 2015; *Madala et al.*, 2015] have shown that there are seasonal variations or discrepancy of various parameterization schemes and this is the inspiration of this work, we would like to insert an effort

to study the seasonal sensitivity of various parameterisation schemes and extrapolate their applicability.

The objective of this study is hence to investigate the performance of the turbulence parameterisation scheme in the WRF mesoscale model of boundary laminar flow structure simulations in the East Asian subtropical region of Yangtze River Delta (YRD) region in China, a city-cluster that has been suffering from serious air pollution in recent years. In particular, we focus on the seasonal discrepancy in the study area and assess the respective skill of four different PBL schemes in reproducing the meteorological variables in different seasons and discuss their respective applicability. This research will provide valuable suggestions regarding more suitable PBL scheme selections in WRF to drive more reasonable air quality simulations

2 Methodology

2.1 WRF configuration

The WRF version 4.0 is employed as the numerical tool in this study. It is a non-hydrostatic mesoscale weather simulation system with flexible resolution and parametric scheme. Initial and lateral boundary conditions are 6 hourly ($1.0^{\circ} \times 1.0^{\circ}$ resolution) Global Final Analysis (FNL) data, provided by the National Center for Environmental Prediction-National Center for Atmospheric Research (NCEP/NCAR). The first 24 h of the simulation period is used as spin-up time and the remaining simulations are computed with a 120 h forecast cycle for analyses for each episodes of study.

In this study, three nested domains are configured, the horizontal grid resolution for domains 1, 2, 3 are 36 km, 12 km, and 4 km, respectively. The coarse D01 (186×149) covers most of the East Asia and part of Southeast Asia, while D02 (148×241) covers east China. D03 (205×229) encompasses the entire YRD region (Fig. 1). The Yangtze Delta is located in the north marine monsoon subtropical climate zone of southeast China. The weather is generally warm and humid in summer and cool and dry in winter. The three domains use the same 39 vertical levels with a model top set at 50-hPa where first 19 layers are from the planetary boundary layer. Simulations are conducted for July and November 2018, started at 0000UTC. The whole month is divided into 6 parts with 5 days concluded. The initial 24 hours are considered as a spin-up period, and the respective outputs during these two periods are excluded from the analysis. The analysis nudging option is switched on above the PBL for the horizontal wind components, potential temperature, and water vapour mixing ratio through three domains.

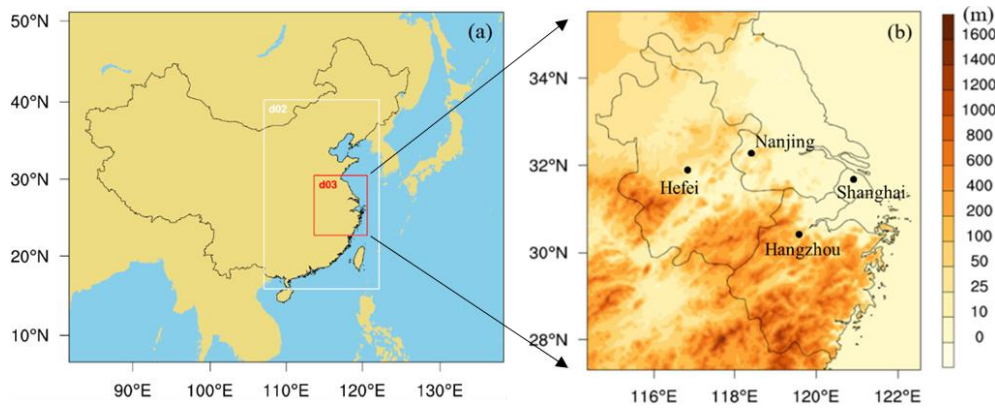


Fig 1. (a) The three nested modeling domains for WRF model and (b) terrain height for the inner Yangtze River Delta (YRD) region

The main physical-parameterisation schemes contain the Lin microphysics scheme [Lin *et al.*, 1983], the NOAH land surface scheme [Chen and Dudhia, 2001], the Kain–Fritsch (KF) cumulus parameterisation (only used in D01 and D02) [Kain and Fritsch, 1993], the rapid radiative transfer model shortwave radiation scheme and the rapid radiative transfer model longwave radiation scheme [Mlawer *et al.*, 1997].

2.2 PBL scheme

Two local and two non-local schemes are implemented in this study. These four models are chosen due to the extensive use in research and are the most commonly used in application [Clark *et al.*, 2015; Deppe *et al.*, 2013; Lo *et al.*, 2008; Steele *et al.*, 2013; Su and Fung, 2015; Yerramilli *et al.*, 2010]. The Yonsei University (YSU) PBL scheme is a first-order non-local closure scheme. Revised from the Medium-Range Forecast (MRF) scheme, the significant improvement to YSU is the addition of an explicit term for the treatment of the entrainment process at the top of YSU. PBL height in the YSU scheme is determined from the Richardson bulk number, with a critical bulk Richardson number of 0.25 over land. This scheme improves the boundary layer diffusion algorithm to allow deeper mixing in windy conditions. Compared to MRF, vertical mixing in the buoyancy driven is increased and in the mechanic driven is decreased [Hong *et al.*, 2006]. However, it also shows weakness in mixing too little over the cold oceans and producing a too low nocturnal PBL height [Hong, 2010].

The ACM2 scheme [Pleim, 2007] is a combination of ACM1 and adds an eddy diffusion component to the non-local transport. It calculates the PBL height above the level of neutral buoyancy by using bulk Richardson number over the critical value of 0.25. ACM2 is intended to better represent the shape of the vertical profiles and be more applicable to humidity, winds, or trace chemical mixing ratios in the boundary layer scheme. It also has defects in showing a deeper

mixing PBL than other schemes due to its larger critical the bulk Richardson number [Huang *et al.*, 2019].

The MYJ scheme [Janjić, 1990] is a one-and-half order local turbulence closure scheme. It diagnoses the vertical mixing process in PBL and free atmosphere through forecasting the TKE, combining with one additional prognostic equation of the TKE. In this method, the upper limit of the main length scale is given, which depends on the turbulence kinetic energy and the shear stress of the buoyancy and driving flow. Under unstable conditions, the equation form of this upper limit is derived from the turbulent kinetic energy during the growth of turbulence satisfying non-singular conditions. By comparison, The MYJ scheme shows moister, cooler and little mixing PBL than other schemes since it has a smaller turbulent mixing [Hu *et al.*, 2010].

The MYNN scheme [Nakanishi and Niino, 2006] is a one-and-half order, local closure scheme. To overcome the biases of insufficient growth of convective boundary layer and under-estimated TKE, MYNN considers the effects of buoyancy in the diagnosis of the pressure covariance terms, and uses closure constants in the stability functions and mixing length formulations that are based on large eddy simulation (LES) results rather than observational datasets. This scheme takes into account the effect of buoyancy on the barometric correlation term and introduces the condensation physics process, and is applied to the study of fog events in general [Chaouch *et al.*, 2017; Li *et al.*, 2012; Román-Cascón *et al.*, 2012].

2.3 Model performance evaluation

The meteorological simulations containing 2-m surface temperature, 10-m wind speed, relative humidity from four capital stations at Shanghai (121.336°N 31.198°E), Hangzhou (120.432°N 30.228°E), Nanjing (118.862°N 31.742°E), Hefei (117.298°N 31.78°E) are compared with the hourly meteorological observations to validate the model. The observational data are obtained from the National Oceanic and Atmospheric Administration (NOAA)'s National Climate Data Center archive (<http://www.ncdc.noaa.gov/oa/ncdc.html>). Meteorology variables are evaluated employing mean bias (MB), root of mean square error (RMSE), and correlation coefficient (R). In statistics, they are usually defined as:

$$\text{MB} = \frac{1}{N} \sum_{i=1}^N (M_i - O_i) ,$$
$$\text{RMSE} = \sqrt{\frac{1}{N} \sum_{i=1}^N (M_i - O_i)^2} ,$$

$$R = \frac{1}{N} \sum_{i=1}^N \frac{(M_i - \bar{M})(O_i - \bar{O})}{\sqrt{\frac{1}{N} \sum_{i=1}^N (M_i - \bar{M})^2} \sqrt{\frac{1}{N} \sum_{i=1}^N (O_i - \bar{O})^2}}$$

where M and O refer to the simulated and observed meteorological values, respectively. N represents the number of data pairs.

3 Results and discussions

3.1 Comparison of surface meteorological variables

The 2-m temperature (T2), 10-m wind speed (WS10) and relative humidity (RH) are critically important variables to precisely predict air quality model simulations and hence these three variables will be used as main indicators for evaluation. Tables 1 and 2 show the MB, RMSE and R between the WRF simulated meteorological factors and the observations at four airport stations in the YRD region. Figures 2, 4 and 6 show the monthly time series of the model predicted and observed meteorology variables. There is a period of missing observation data in late November.

3.1.1 2-m temperature

Aside from the fact that all four PBL schemes have different degrees of overestimation around 6 July, the simulated 2-m temperatures are generally consistent with the observed trends, which is usual for most temperature WRF-simulations [Giannaros *et al.*, 2013; Hogrefe *et al.*, 2015; Mallard *et al.*, 2014; Mughal *et al.*, 2019; Wang *et al.*, 2017b]. In terms of individual cases over the summer in particular, except the local-closure MYJ scheme, other three schemes underestimate 2-m temperature in Shanghai, while four PBL schemes slightly overestimate 2-m temperature in Hefei. All four PBL schemes underestimate 2-m temperature in Nanjing and Hangzhou. The YSU and ACM2 schemes perform better than the MYJ and MYNN schemes at 2-m temperature with the least RMSE (2.55, 2.32, 2.73 and 2.56 °C for YSU, ACM2, MYJ and MYNN scheme) (Table 1). In general, the simulations of summer temperature are higher than the observations. Shin and Hong [2011] also reports positive biases with the different PBL schemes. The average observed temperature in summer is 29.92°C and the average of ACM2 scheme is closest to the observation with 29.93°C. In terms of RMSE and correlation coefficient in summer, ACM2 scheme is also better than other schemes. The temporal series of the WRF model-simulated meteorological variables against observations from the four meteorological stations of July is shown in Fig. 2a. It is reasonable to infer that the monthly overestimation of simulated 2-m temperature of four PBL schemes at Hefei is in large part due to a notable overestimation in the early and mid-July. Among which the MYJ scheme provides the highest bias. All four PBL schemes provide some overestimations at the beginning of July.

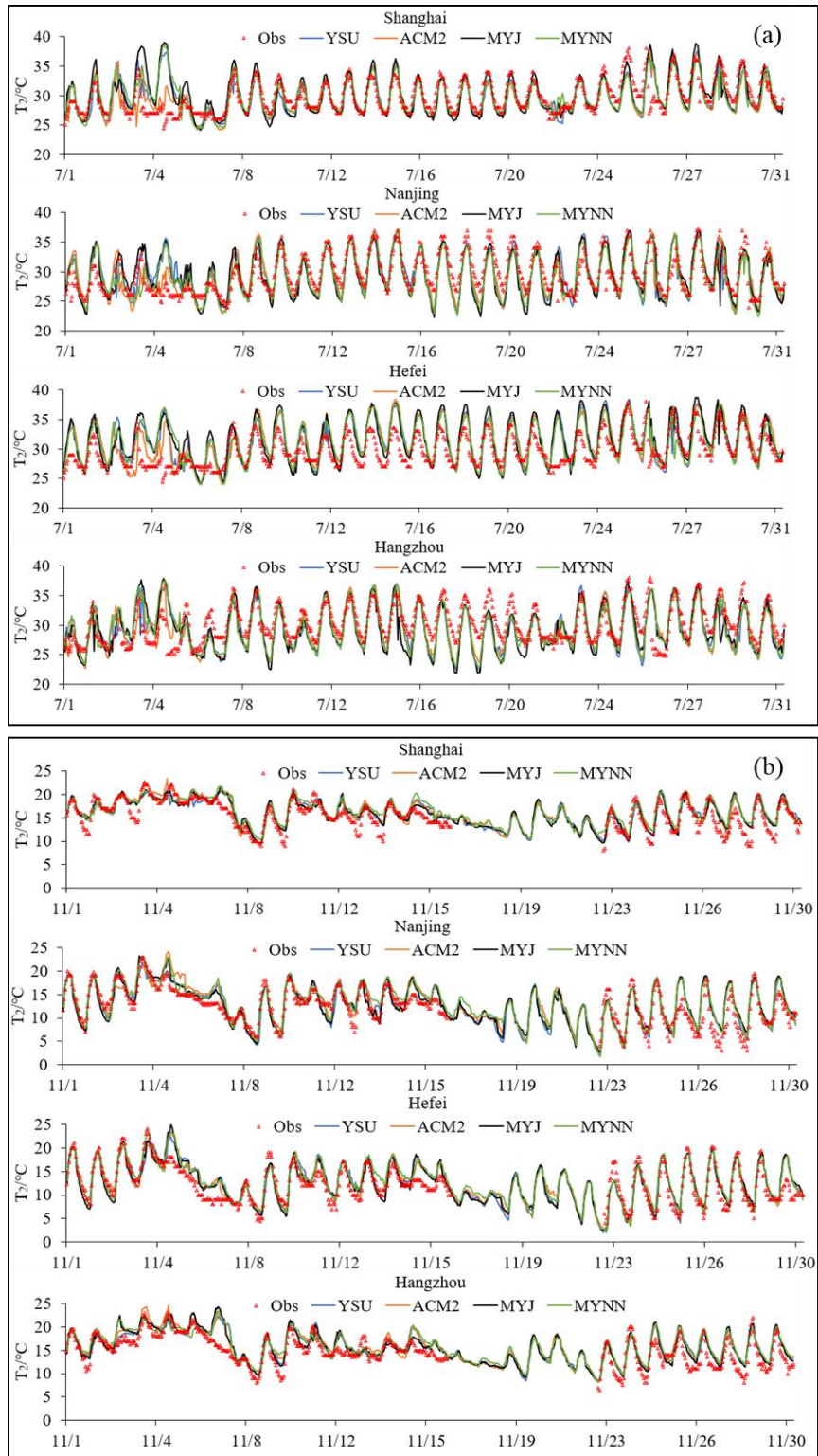
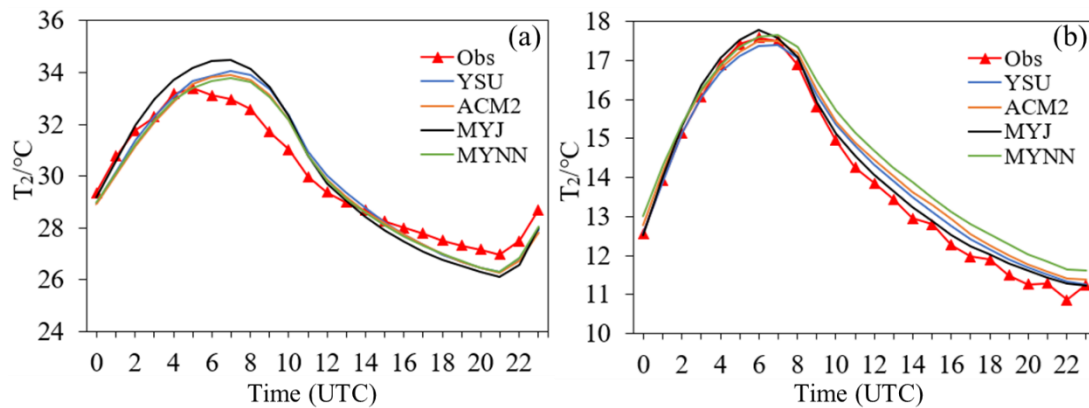


Fig 2. Comparisons of the time series of 2-m temperature predicted with WRF against observations at four sites for summer (a) and winter (b).

Different from the case of summer, simulations of the four PBL schemes for 2-m temperature are overestimated at all sites in winter (Fig. 2b). The main reason is that the boundary layer is mostly in a steady stable state in winter, and coupled with the influence of complex topography, strong

inversion temperature, insufficient development of turbulence in the near-surface layer, and the transport of material and energy is dominated by the local area. The MYNN scheme overestimates the most among all simulations. In Shanghai, the YSU scheme shows the lowest MB of 0.83 °C, the ACM2 and MYJ schemes perform slightly better with high correlation coefficient with 0.87 (Table 2). Though the simulations of the YSU, ACM2 and MYJ schemes are close, 2-m temperature simulations of local closure MYJ scheme are better than those of non-local closure YSU and ACM2 schemes. Simulated 2-m temperature deviation in winter with MB is greater than that in summer while the consistency of winter is much better than summer on the whole. This is probably due to the lower temperature in winter and the smaller amplitude variation brought about by the simulation compared to summer.

Comparing the average diurnal changes of 2-m temperature, it can be seen that all four PBL schemes could reflect the diurnal variations reasonably well (Fig. 3). Due to the different treatment of physical processes in the boundary layer, even if the same land surface parameters are used, the difference in surface turbulence transportation will cause significant discrepancies in the simulated surface temperature of the four experiments [Lee *et al.*, 2006]. In summer, the daytime simulations of T2 are generally higher than the observations, but lower than observations at night. On the contrary, during winter night, the simulations exhibit overestimation. The main reason for the overestimation in summer daytime is that the YRD region is located in the intersection zone of land and sea. Under the influence of the summer monsoon, the water vapour transport is stronger in the daytime, resulting in stronger water vapor transport. A small cold bias is observed during the summer night which may attribute to an overestimation of the surface cooling rate during the PBL collapse. Similar finding is also reported by Cuchiara *et al.* [2014]. The surface temperature simulated by the local closure MYJ scheme during winter night is better than that simulated by the non-local closure YSU and ACM2 schemes. The boundary layer is in a steady state during winter, especially due to the influence of valley topography with strong inversion temperature, near-surface turbulence is not fully developed, material and energy transport are mainly local.



3.1.2 10-m wind speed

All four PBL schemes overestimate 10 m-wind speed over the YRD region (Fig. 4), however, there are some differences among the cities due to their specific locations. Different from Shanghai, located along the coastline, the other three sites are all located in inner YRD region, closer to the western or southern hills. The WRF model is unable to capture this special geographical environment as well as sub-grid scale local fluctuations, resulting in the overestimations. *Jiménez et al.* [2012] also reports that wind speed was overestimated in the plains and valleys. The ACM2, the MYNN and the YSU schemes underestimate 10 m-wind speed at Shanghai, while the MYJ scheme shows overestimation. Four PBL schemes exhibit overestimation in the other three cities. Among them, the MYNN scheme is the least underestimated with the lowest MB of 0.38 m s^{-1} in summer (Table 1) and 0.17 m s^{-1} in winter (Table 2). Other studies also have shown a general tendency of overestimation regarding the 10-m wind speed simulation [*Cheng et al.*, 2005; *Mölders*, 2008]. The discrepancies in wind speed simulation from the different schemes may be caused by different mixing lengths due to different turbulence coefficients and friction velocities for each scheme.

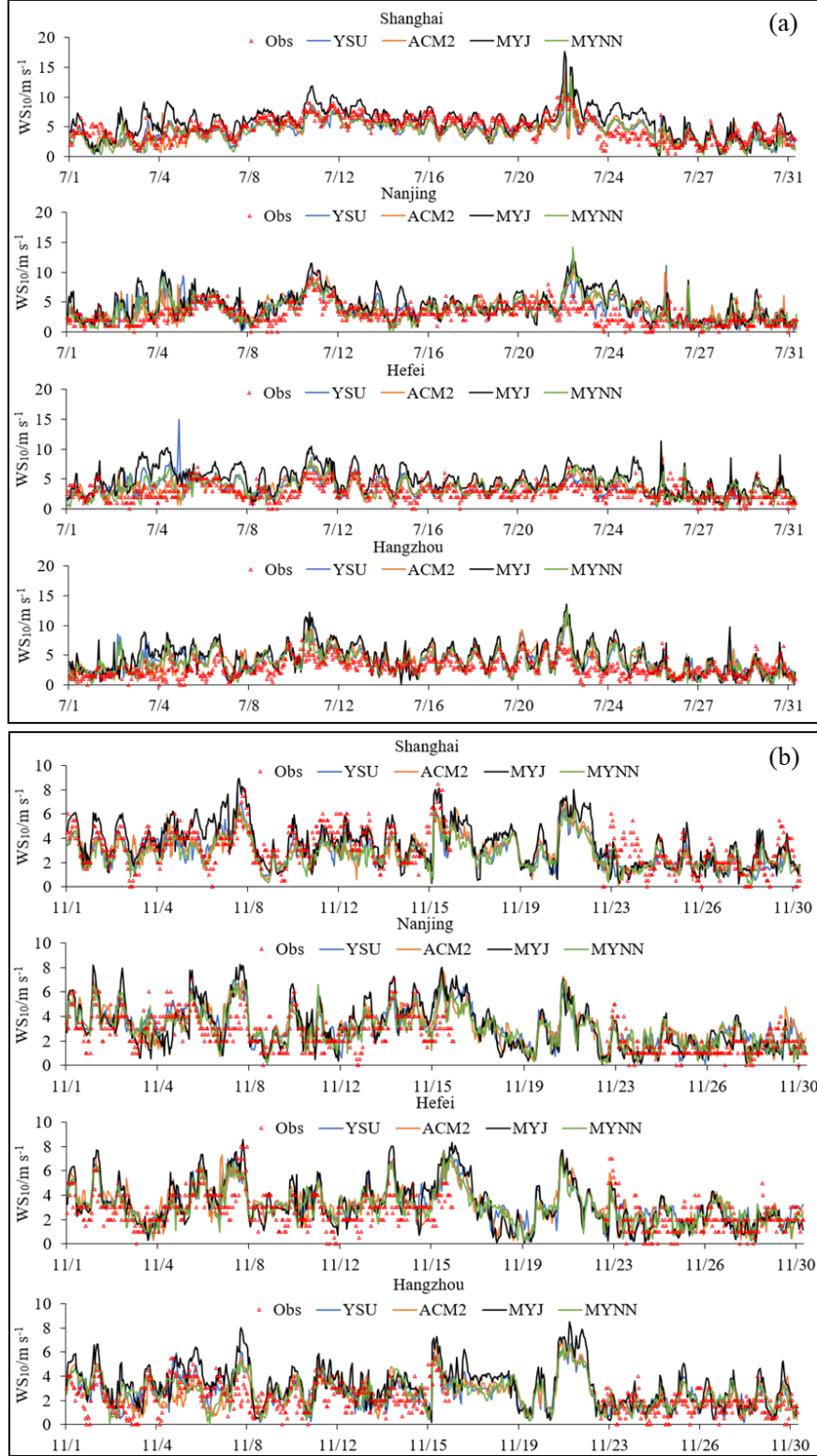


Fig 4. Comparisons of the time series of 10-m wind speed predicted with WRF against observations at four sites for summer (a) and winter (b).

Similar to July, all four PBL schemes overestimate 10 m-wind speed at Nanjing, Hangzhou and Hefei in November, but the gap becomes lower. Relative to the lower consistency of Hefei

simulations in summer, the overall consistency of the winter simulations is better, with all correlation coefficient higher than 0.54. Wind speed fluctuates more in summer than in winter, both physically and also in simulations. Among the four PBL schemes, the MYJ scheme produces the most obvious level of fluctuations. The 10-m wind speed simulations in winter are much closer to observations than summer, and all four PBL parameters perform much better compared to the summer simulations. Seasonal diurnal variation also corresponds to the good performance of ACM2 and MYNN (Fig. 5). Simulations in winter are close to the observations before 0800UTC, and higher than observations after 0800UTC (Fig. 5b). The reason is partly due to the overestimation of the surface friction velocity at night. The MYNN2 scheme provides the lowest bias throughout the day and night hours in summer as well as these night hours in winter. This is expected since the MYNN is based on local closure, which is better suited for stable conditions prevailing in winter. This may also be due to higher diffusivity coefficients simulated by ACM2 and MYNN [Hariprasad *et al.*, 2014], which exhibit lower wind speed and subsequent less errors compared with other schemes.

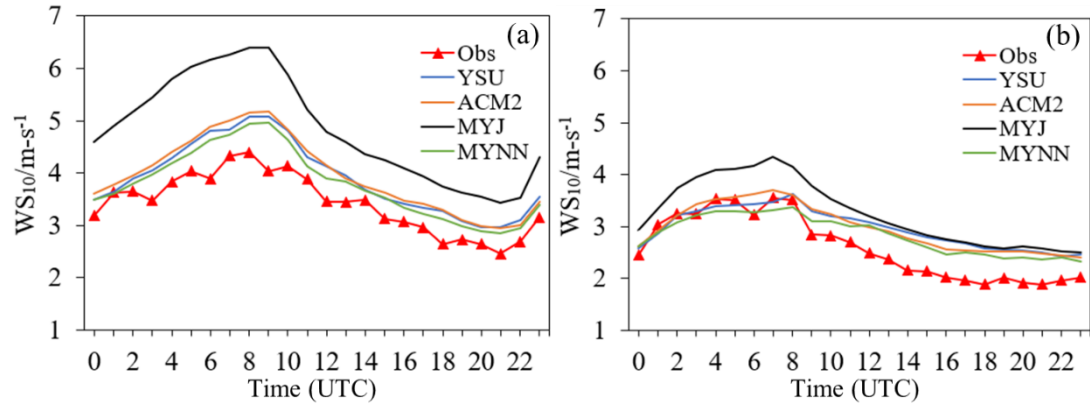


Fig 5. Average diurnal changes of 10-m wind speed for summer (a) and winter (b).

3.1.3 Relative humidity

As for relative humidity, all four PBL schemes mostly exhibit underestimations. Underestimation of humidity by MYJ and YSU schemes is also reported by *Misenis and Zhang* [2010] in air quality simulations over the coastal Mississippi. It can be seen from Table 1 and 2 that ACM2 scheme shows the lowest MB of -4.86 and highest correlation coefficient of 0.71 in summer (Fig. 6a), MYJ scheme provides the lowest MB of -5.86 and relatively good correlation coefficient of 0.69 in winter (Fig. 6b). The underestimation of humidity is greater in winter than that in summer. This may be attributed to the moisture content of the atmosphere, which is inherently small in winter, and the diurnal temperature variation becomes the dominant factor in relative humidity changes. In winter, due to weak mixing and clamping, the relative humidity simulation of MYJ scheme is higher than the other schemes.

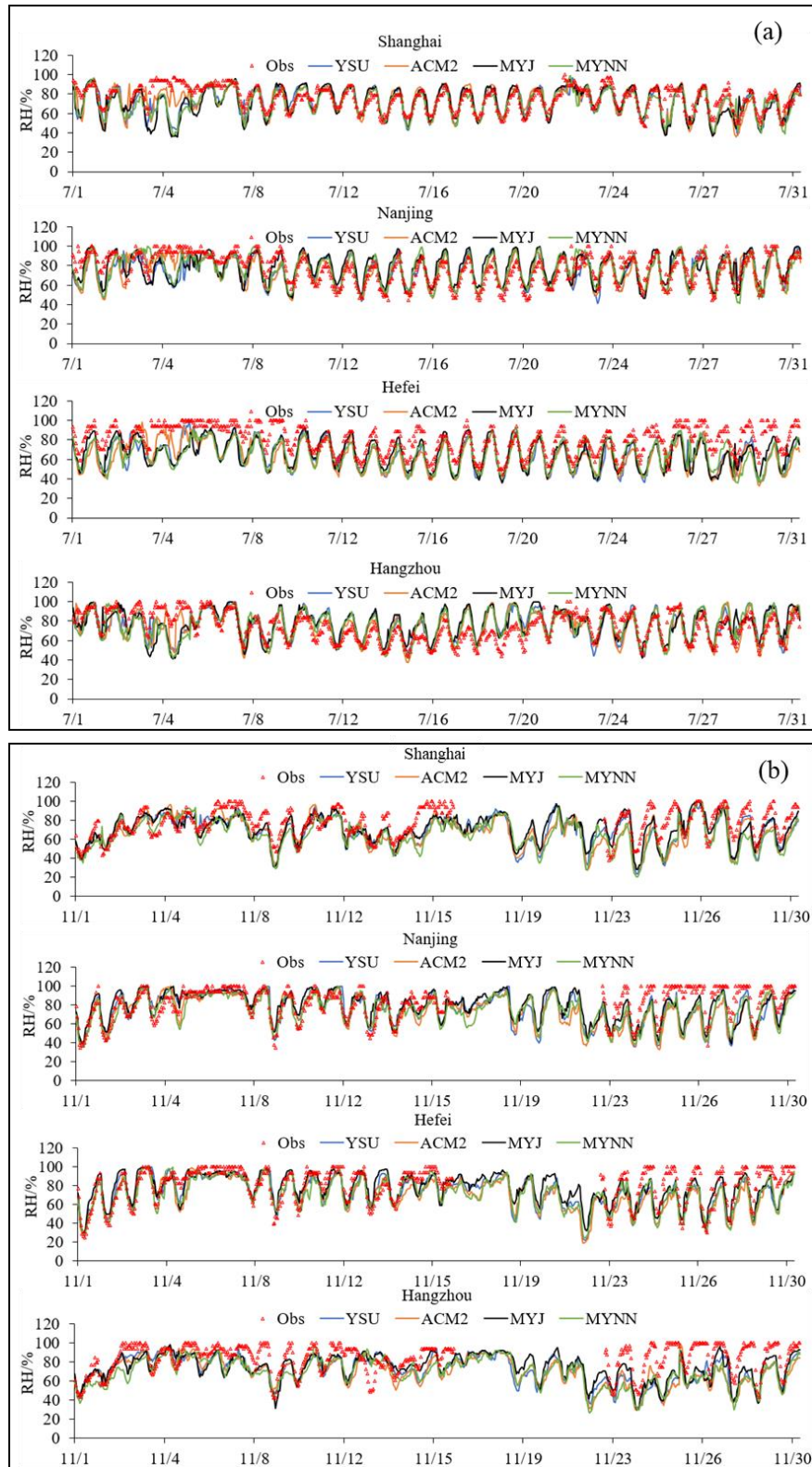


Fig 6. Comparisons of the time series of relative humidity predicted with WRF against observations at four sites for summer (a) and winter (b).

The diurnal relative humidity variation is relatively well reproduced with all PBL schemes.

Relative humidity is not an output of the model but inferred from some variables of temperature, water vapour mixing ratio, and surface pressure. During daytime in summer, strong underestimation is shown with all PBL schemes and dry bias becomes smaller in night hours (Fig. 7a). It is seen that ACM2 simulates the relative humidity better. In winter, all PBL schemes provide dry bias during day and night hours (Fig. 7b). *Gunwani and Mohan* [2017] also reports that in temperate zone higher dry bias is modeled by all PBL schemes compared to other climate zones.

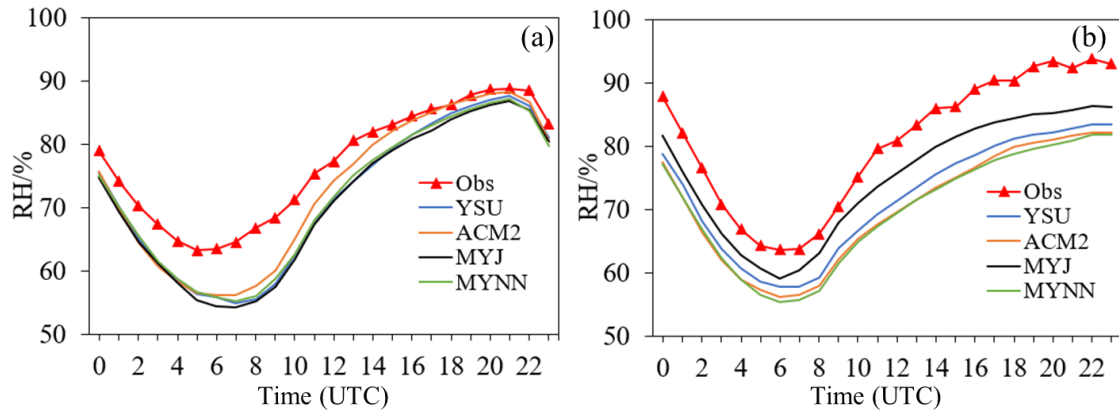


Fig 7. Average diurnal changes of relative humidity for summer (a) and winter (b).

3.2 Comparison of PBL height

3.2.1 Temporal variations of PBL height

One of the largest sources of errors in mesoscale model simulations is the diagnosis of the PBL height. Estimates of the hourly PBL height between 0800 and 1700LST are determined based on observations from a micropulse lidar (MPL) at Hefei Environmental Protection Bureau (31.78 N, 117.20 E). Due to the instrument limitations, the PBL height at night and early morning is not considered. Figure 8a shows hourly average PBL heights estimated from the MPL on 18 July 2018. The mean PBL height for the day is 1.46 km with a small aerosol extinction. Based on the available hourly PBL data, the WRF model simulations are compared.

Figure 8b compares the hourly average results in the daytime from MPL to the PBL heights simulated by the WRF model. It is noted that in general the WRF model systematically underestimates the PBL height. The MYJ scheme leads to the most underestimation with MB of -0.51 km. The ACM2 scheme exhibits the lowest MB of 0.12 km. As for the daytime-maximum PBL heights, the ACM2 also shows the lowest discrepancies compared to the MPL estimate with 0.07 km. The MYNN scheme shows an optimal performance in which the correlation coefficient

was 0.90 and the ACM2 scheme demonstrates relatively a good result with 0.88. Fig. 8c provides time-series comparisons for July of four PBL schemes simulations to the lidar measurement. Due to limitation of data acquisition, some dates occur data missing. The strong diurnal daytime PBL patterns are captured in all four experiments especially for the MYJ scheme, however, four schemes exhibit varying degrees of overestimations at daytime-maximum PBL height. For comparison of the data available, the MYNN exhibits the lowest MB of 0.04 km and the ACM2 scheme shows the highest correlation coefficient of 0.59.

378 Table 1 Statistics of WRF model performance with different PBL schemes in July, 2018

379	Shanghai			Nanjing			Hangzhou			Hefei			Average		
	MB	RMSE	R	MB	RMSE	R	MB	RMSE	R	MB	RMSE	R	MB	RMSE	R
	$T_2/^{\circ}\text{C}$														
YSU	-0.15	2.17	0.69	-0.06	2.38	0.76	-0.74	2.64	0.71	1.77	2.99	0.78	0.20	2.55	0.72
ACM2	-0.35	1.80	0.79	-0.27	2.10	0.81	-0.70	2.33	0.77	1.72	3.03	0.77	0.10	2.32	0.77
MYJ	0.25	2.49	0.68	-0.26	2.41	0.76	-0.91	2.76	0.71	2.03	3.25	0.76	0.28	2.73	0.72
MYNN	-0.06	2.32	0.63	-0.42	2.21	0.80	-0.85	2.33	0.70	1.67	3.01	0.77	0.09	2.56	0.71
	WS_{10}/ms^{-1}														
YSU	-0.46	1.52	0.70	0.81	1.90	0.54	0.96	1.90	0.54	0.64	1.68	0.29	0.49	1.75	0.55
ACM2	-0.45	1.49	0.71	0.98	2.01	0.55	1.12	1.95	0.59	0.55	1.56	0.30	0.55	1.75	0.58
MYJ	1.03	2.20	0.62	1.33	2.48	0.52	1.46	2.55	0.51	1.89	2.68	0.27	1.43	2.48	0.53
MYNN	-0.60	1.55	0.71	0.71	2.01c	0.48	0.77	1.80	0.56	0.64	1.64	0.29	0.38	1.75	0.58
	$\text{RH}/\%$														
YSU	-3.76	11.13	0.67	-2.54	12.12	0.68	1.39	12.80	0.61	-16.20	19.37	0.67	-5.28	13.86	0.66
ACM2	-2.62	9.70	0.76	-1.32	11.14	0.74	-0.29	11.50	0.70	-15.22	18.11	0.64	-4.86	12.61	0.71
MYJ	-4.76	13.22	0.59	-0.98	12.07	0.66	1.22	13.75	0.55	-15.52	18.35	0.67	-5.01	14.35	0.62
MYNN	-5.16	11.68	0.65	-1.00	10.97	0.73	1.33	12.61	0.63	-16.03	19.56	0.64	-5.22	13.71	0.66

	SH			NJ			HZ			HF			Ave		
	MB	RMSE	R	MB	RMSE	R	MB	RMSE	R	MB	RMSE	R	MB	RMSE	R
T ₂ /°C															
YSU	0.83	1.80	0.85	0.68	2.12	0.87	1.23	2.13	0.60	0.83	2.07	0.89	0.89	2.03	0.86
ACM2	0.91	1.73	0.87	0.88	2.26	0.86	1.40	2.22	0.61	0.80	2.00	0.89	1.00	2.05	0.87
MYJ	0.84	1.70	0.87	0.67	2.10	0.87	1.22	2.08	0.65	0.68	2.12	0.87	0.28	2.00	0.87
MYNN	1.24	2.08	0.84	1.00	2.17	0.88	1.51	2.37	0.50	1.01	2.15	0.89	1.19	2.19	0.86
WS ₁₀ /m·s ⁻¹															
YSU	-0.34	1.35	0.60	0.60	1.35	0.66	0.33	1.23	0.62	0.56	1.41	0.55	0.28	1.33	0.57
ACM2	-0.31	1.39	0.56	0.62	1.43	0.62	0.29	1.28	0.57	0.53	1.46	0.54	0.28	1.39	0.54
MYJ	0.28	1.49	0.62	0.57	1.61	0.62	0.90	1.64	0.58	0.56	1.57	0.60	0.58	1.58	0.59
MYNN	-0.54	1.41	0.59	0.45	1.31	0.63	0.38	1.30	0.56	0.38	1.35	0.55	0.17	1.34	0.57
RH/%															
YSU	-8.52	15.11	0.66	-6.21	14.82	0.67	-12.50	18.90	0.77	-6.78	13.03	0.80	-8.50	15.46	0.67
ACM2	-8.74	15.34	0.67	-8.26	15.85	0.66	-14.35	20.32	0.76	-8.81	14.67	0.78	-10.04	16.55	0.66
MYJ	-6.66	13.21	0.71	-3.23	13.06	0.68	-10.56	16.81	0.80	-3.01	11.85	0.78	-5.86	13.73	0.69
MYNN	-12.42	17.75	0.66	-8.12	14.25	0.74	-15.50	20.77	0.75	-8.09	12.87	0.84	-11.03	16.41	0.70

380 Table 2 Statistics of WRF model performance with different PBL schemes in November, 2018

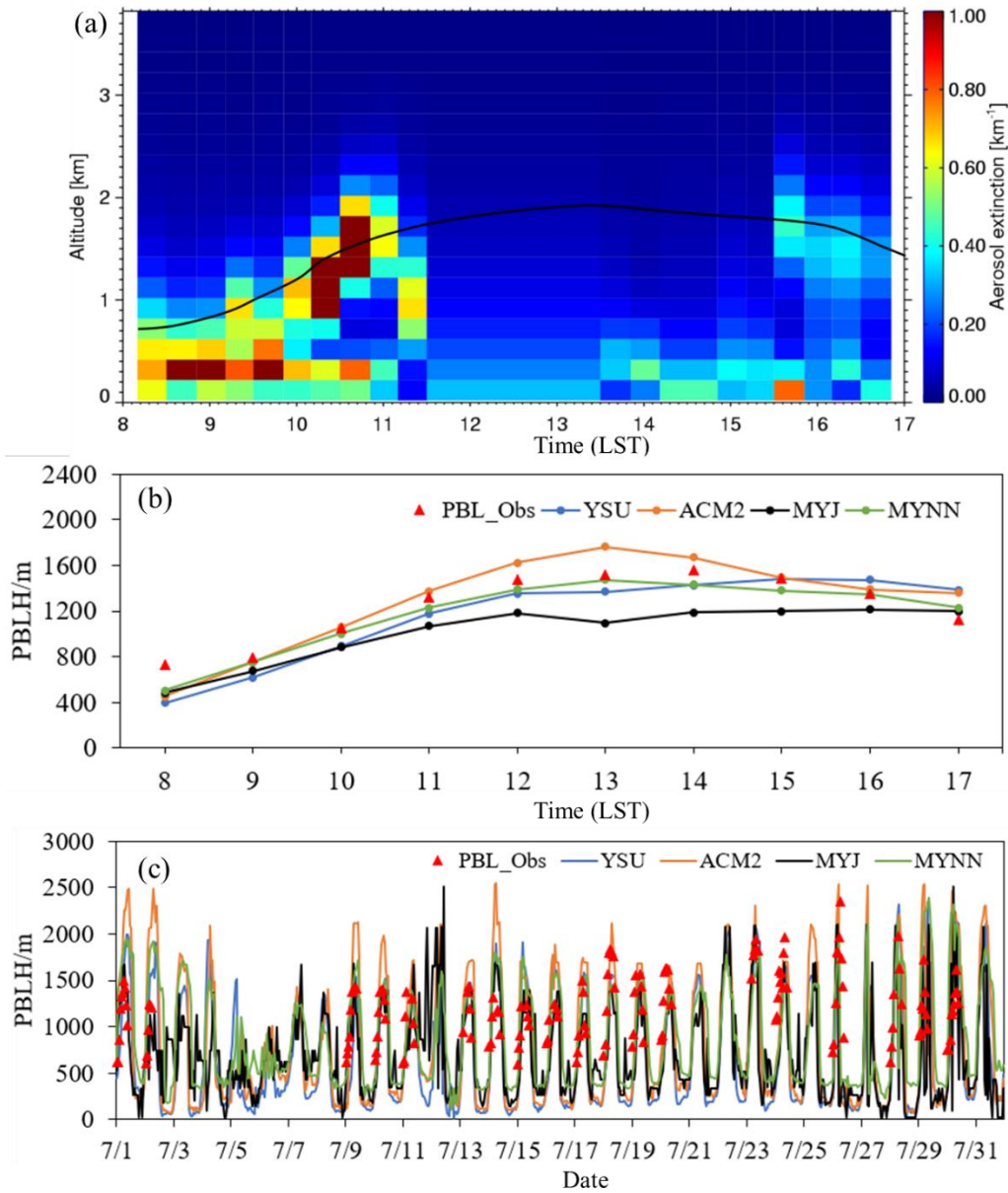


Fig 8. (a) Time-series of aerosol extinction, overlaid with hourly PBL heights. (b) Time series of daytime PBL heights simulations and hourly average from the lidar on 18 July 2018. (c) Time series of monthly PBL heights simulated by WRF and available hourly average from the lidar of July 2018.

4 Conclusions

In this study, a seasonal sensitivity analysis study from the Weather Research and Forecasting (WRF) mesoscale model is conducted to explore the impacts of four most commonly used PBL schemes (YSU, ACM2, MYJ and MYNN) on meteorological variables over the YRD region. The WRF simulation indicates that all the four PBL schemes overestimate the 2-m temperature ($0.09\sim 0.20^{\circ}\text{C}$ for July; $0.28\sim 1.19^{\circ}\text{C}$ for November) and 10-m wind speed ($0.38\sim 1.43\text{m/s}$ for July; $0.17\sim 0.58\text{m/s}$ for November), underestimate the relative humidity ($-4.07\sim -5.86\%$ for July;

-5.86%~-11.03% for November). Warm bias in summer is mostly shown in daytime, mainly as a consequence of overestimated breeze circulations. The warm deviation in winter is possibly related to the unresolved strong temperature inversion and the stability limitation of surface parameterisation. Wind speed of overestimation in summer is higher than winter.

Diagnosis of the surface level meteorological variables indicate that for temperature the non-local closure scheme ACM2 simulated well in summer while MYJ performs better in winter. For wind speed, ACM2 scheme and the local closure scheme MYNN produced better simulations, and the MYJ and YSU schemes slightly overestimated the winds than the formers. For humidity, ACM2 and YSU schemes simulate reasonably well in summer and relatively underestimated in winter while the other three schemes produced close simulations and the MYNN performed larger bias in winter. Generally, the simulations of winter cases are better than that of summer cases, the reason is related to the relatively stable flow field in winter. ACM2 performs better in meteorological factors than other three schemes in summer and MYJ provides better simulations in winter.

Comparisons of the PBL heights reveal that all four PBL schemes show varying degrees of underestimation, with the MYJ scheme exhibited the largest underestimation and the ACM2 scheme the smallest. All four schemes capture a strong diurnal PBL pattern of daily variation while the MYNN scheme performed the lowest MB and the ACM2 scheme provided the highest correlation coefficient.

In summary, we find that model systematic errors are dependent on the seasonal and daily cycles, and variable terrain conditions that causes different atmospheric factors. The non-local PBL scheme ACM2 performs well for model simulations of the meteorology and PBL height in summer while the local PBL scheme exhibits better simulation results in winter over YRD region.

Acknowledgement

This study is financially supported by the National Natural Science Foundation of China (NO. 42075144, 41875161, 42005112), Shanghai International Science and Technology Cooperation Fund (NO. 19230742500), the National Key R&D Program of China (NO.2018YFC0213600), the Shanghai Science and Technology Innovation Plan (NO.19DZ1205007), and the Shanghai Sail Program (No. 19YF1415600). We thank Prof. Liu Cheng at University of Science and Technology of China for helping with derivation of the PBL data from Lidar measurement.

References

- Ayotte, K. W., P. P. Sullivan, A. Andren, S. C. Doney, A. A. Holtslag, W. G. Large, J. C. McWilliams, C.-H. Moeng, M. J. Otte, and J. Tribbia (1996), An evaluation of neutral and convective planetary boundary-layer parameterizations relative to large eddy simulations, *Boundary-Layer Meteorology*, 79(1-2), 131-175.
- Banks, R. F., and J. M. Baldasano (2016), Impact of WRF model PBL schemes on air quality simulations over Catalonia, Spain, *Science of the total environment*, 572, 98-113.
- Bright, D. R., S. L. Mullen (2002), The sensitivity of the numerical simulation of the southwest monsoon boundary layer to the choice of PBL turbulence parameterization in MM5, *Weather and Forecasting*, 17(1), 99-114.
- Bryan, G. H., J. C. Wyngaard, and J. M. Fritsch (2003), Resolution requirements for the simulation of deep moist convection, *Monthly Weather Review*, 131(10), 2394-2416.
- Chaouch, N., M. Temimi, M. Weston, and H. Ghedira (2017), Sensitivity of the meteorological model WRF-ARW to planetary boundary layer schemes during fog conditions in a coastal arid region, *Atmospheric Research*, 187, 106-127.
- Chen, F., and J. Dudhia (2001), Coupling an advanced land surface-hydrology model with the Penn State-NCAR MM5 modeling system. Part I: Model implementation and sensitivity, *Monthly weather review*, 129(4), 569-585.
- Cheng, W. Y., W. J. Steenburgh, (2005), Evaluation of surface sensible weather forecasts by the WRF and the Eta models over the western United States, *Weather and Forecasting*, 20(5), 812-821.
- Chu, Y., J. Li, C. Li, W. Tan, T. Su, and J. Li (2019), Seasonal and diurnal variability of planetary boundary layer height in Beijing: Intercomparison between MPL and WRF results, *Atmospheric research*, 227, 1-13.
- Clark, A. J., M. C. Coniglio, B. E. Coffey, G. Thompson, M. Xue, F. Kong, (2015), Sensitivity of 24-h forecast dryline position and structure to boundary layer parameterizations in convection-allowing WRF Model simulations, *Weather and Forecasting*, 30(3), 613-638.
- Cohen, A. E., S. M. Cavallo, M. C. Coniglio, H. E. Brooks, (2015), A review of planetary boundary layer parameterization schemes and their sensitivity in simulating southeastern US cold season severe weather environments, *Weather and forecasting*, 30(3), 591-612.
- Coniglio, M. C., J. Correia Jr, P. T. Marsh, F. Kong, (2013), Verification of convection-allowing WRF model forecasts of the planetary boundary layer using sounding observations, *Weather and Forecasting*, 28(3), 842-862.
- Cuchiara, G. C., X. Li, J. Carvalho, and B. Rappenglück (2014), Intercomparison of planetary boundary layer parameterization and its impacts on surface ozone concentration in the WRF/Chem model for a case study in Houston/Texas, *Atmospheric Environment*, 96, 175-185.
- Deppe, A. J., W. A. Gallus Jr, E. S. Takle, (2013), A WRF ensemble for improved wind speed forecasts at turbine height, *Weather and Forecasting*, 28(1), 212-228.
- Draxl, C., A. N. Hahmann, A. Peña, and G. Giebel (2014), Evaluating winds and vertical wind shear from Weather Research and Forecasting model forecasts using seven planetary boundary layer schemes, *Wind Energy*, 17(1), 39-55.
- García-Díez, M., J. Fernández, L. Fita, and C. Yagüe (2013), Seasonal dependence of WRF model biases and sensitivity to PBL schemes over Europe, *Quarterly Journal of the Royal Meteorological*

Society, 139(671), 501-514.

Garratt, J. R. (1994), The atmospheric boundary layer, *Earth-Science Reviews*, 37(1-2), 89-134.

Giannaros, T. M., D. Melas, I. A. Daglis, I. Keramitsoglou, and K. Kourtidis (2013), Numerical study of the urban heat island over Athens (Greece) with the WRF model, *Atmospheric Environment*, 73, 103-111.

Gopalakrishnan, S. G., F. Marks Jr, J. A. Zhang, X. Zhang, J.-W. Bao, and V. Tallapragada (2013), A study of the impacts of vertical diffusion on the structure and intensity of the tropical cyclones using the high-resolution HWRF system, *Journal of the atmospheric sciences*, 70(2), 524-541.

Gunwani, P., and M. Mohan (2017), Sensitivity of WRF model estimates to various PBL parameterizations in different climatic zones over India, *Atmospheric Research*, 194, 43-65.

Han, Z., H. Ueda, and J. An (2008), Evaluation and intercomparison of meteorological predictions by five MM5-PBL parameterizations in combination with three land-surface models, *Atmospheric Environment*, 42(2), 233-249.

Hariprasad, K., C. V. Srinivas, A. B. Singh, S. V. B. Rao, R. Baskaran, and B. Venkatraman (2014), Numerical simulation and intercomparison of boundary layer structure with different PBL schemes in WRF using experimental observations at a tropical site, *Atmospheric Research*, 145, 27-44.

Hogrefe, C., G. Pouliot, D. Wong, A. Torian, S. Roselle, J. Pleim, and R. Mathur (2015), Annual application and evaluation of the online coupled WRF-CMAQ system over North America under AQMEII phase 2, *Atmospheric Environment*, 115, 683-694.

Holt, T., and S. Raman (1988), A review and comparative evaluation of multilevel boundary layer parameterizations for first-order and turbulent kinetic energy closure schemes, *Reviews of geophysics*, 26(4), 761-780.

Hong, S.-Y., Y. Noh, and J. Dudhia (2006), A new vertical diffusion package with an explicit treatment of entrainment processes, *Monthly weather review*, 134(9), 2318-2341.

Hong, S. Y. (2010), A new stable boundary-layer mixing scheme and its impact on the simulated East Asian summer monsoon, *Quarterly Journal of the Royal Meteorological Society*, 136(651), 1481-1496.

Hu, X.-M., J. W. Nielsen-Gammon, F. Zhang, (2010), Evaluation of three planetary boundary layer schemes in the WRF model, *Journal of Applied Meteorology and Climatology*, 49(9), 1831-1844.

Huang, M., Z. Gao, S. Miao, F. Chen, (2019), Sensitivity of urban boundary layer simulation to urban canopy models and PBL schemes in Beijing, *Meteorology and Atmospheric Physics*, 131(5), 1235-1248.

Janjić, Z. I. (1990), The step-mountain coordinate: Physical package, *Monthly Weather Review*, 118(7), 1429-1443.

Jia, W., and X. Zhang (2020), The role of the planetary boundary layer parameterization schemes on the meteorological and aerosol pollution simulations: A review, *Atmospheric Research*, 239, 104890.

Jiménez, P. A., J. Dudhia, (2012), Improving the representation of resolved and unresolved topographic effects on surface wind in the WRF model, *Journal of Applied Meteorology and Climatology*, 51(2), 300-316.

Kain, J. S., and J. M. Fritsch (1993), Convective parameterization for mesoscale models: The Kain-Fritsch scheme, in *The representation of cumulus convection in numerical models*, edited, pp. 165-170, Springer.

Kala, J., J. Andrys, T. J. Lyons, I. J. Foster, and B. J. Evans (2015), Sensitivity of WRF to driving data and physics options on a seasonal time-scale for the southwest of Western Australia, *Climate Dynamics*, 44(3-4), 633-659.

Kwun, J. H., Y.-K. Kim, J.-W. Seo, J. H. Jeong, and S. H. You (2009), Sensitivity of MM5 and WRF mesoscale model predictions of surface winds in a typhoon to planetary boundary layer parameterizations, *Natural Hazards*, 51(1), 63-77.

Lee, S.-m., W. Giori, M. Princevac, and H. Fernando (2006), Implementation of a stable PBL turbulence parameterization for the mesoscale model MM5: nocturnal flow in complex terrain, *Boundary-layer meteorology*, 119(1), 109-134.

Li, P., G. Fu, C. Lu, D. Fu, S. Wang, (2012), The formation mechanism of a spring sea fog event over the Yellow Sea associated with a low-level jet, *Weather and Forecasting*, 27(6), 1538-1553.

Li, T., H. Wang, T. Zhao, M. Xue, Y. Wang, H. Che, and C. Jiang (2016), The impacts of different PBL schemes on the simulation of PM_{2.5} during severe haze episodes in the Jing-Jin-Ji region and its surroundings in China, *Advances in Meteorology*, 2016.

Lin, Y.-L., R. D. Farley, H. D. Orville, (1983), Bulk parameterization of the snow field in a cloud model, *Journal of Climate Applied Meteorology*, 22(6), 1065-1092.

Lo, J. C. F., Z. L. Yang, and R. A. Pielke Sr (2008), Assessment of three dynamical climate downscaling methods using the Weather Research and Forecasting (WRF) model, *Journal of Geophysical Research: Atmospheres*, 113(D9).

Madala, S., A. Satyanarayana, C. Srinivas, and M. Kumar (2015), Mesoscale atmospheric flow-field simulations for air quality modeling over complex terrain region of Ranchi in eastern India using WRF, *Atmospheric Environment*, 107, 315-328.

Mallard, M. S., C. G. Nolte, O. R. Bullock, T. L. Spero, and J. Gula (2014), Using a coupled lake model with WRF for dynamical downscaling, *Journal of Geophysical Research: Atmospheres*, 119(12), 7193-7208.

Misenis, C., and Y. Zhang (2010), An examination of sensitivity of WRF/Chem predictions to physical parameterizations, horizontal grid spacing, and nesting options, *Atmospheric Research*, 97(3), 315-334.

Mlawer, E. J., S. J. Taubman, P. D. Brown, M. J. Iacono, and S. A. Clough (1997), Radiative transfer for inhomogeneous atmospheres: RRTM, a validated correlated-k model for the longwave, *Journal of Geophysical Research: Atmospheres*, 102(D14), 16663-16682.

Moeng, C.-H. J. J. o. t. A. S. (1984), A large-eddy-simulation model for the study of planetary boundary-layer turbulence, *Journal of the Atmospheric Sciences*, 41(13), 2052-2062.

Mohan, M., and S. J. A. i. M. Bhati (2011), Analysis of WRF model performance over subtropical region of Delhi, India, *Advances in Meteorology*, 2011.

Mölders, N. (2008), Suitability of the Weather Research and Forecasting (WRF) model to predict the June 2005 fire weather for Interior Alaska, *Weather and Forecasting*, 23(5), 953-973.

Mughal, M. O., X. X. Li, T. Yin, A. Martilli, O. Brousse, M. A. Dissegna, and L. K. Norford (2019), High-Resolution, Multilayer Modeling of Singapore's Urban Climate Incorporating Local Climate Zones, *Journal of Geophysical Research: Atmospheres*, 124(14), 7764-7785.

Nakanishi, M., and H. Niino (2006), An improved Mellor–Yamada level-3 model: Its numerical stability and application to a regional prediction of advection fog, *Boundary-Layer Meteorology*, 119(2), 397-407.

Ooi, M.C.G., Chan, A., Subramaniam, K., Morris, K.I. & Oozeerm, M.Y. (2018), Interactions of Urban Heating and Local Winds During the Calm Intermonsoon Seasons in the Tropics, *Journal of Geophysical Research: Atmospheres*, 122(11), 11499-11523.

Oozeer, M.Y. Chan, A., Ooi, M.C.G., Zarzur, A.M., Salinas, S.V., Chew, B.N., Morris, K.I., & Choong, W.K. (2016), Numerical study of the transport and convective mechanisms of biomass burning haze in

South-Southeast Asia, *Aerosol and Air Quality Research*, 16, 2950-2963

Penchah, M. M., H. Malakooti, and M. Satkin (2017), Evaluation of planetary boundary layer simulations for wind resource study in east of Iran, *Renewable Energy*, 111, 1-10.

Pleim, J. E. (2007), A combined local and nonlocal closure model for the atmospheric boundary layer. Part I: Model description and testing, *Journal of Applied Meteorology and Climatology*, 46(9), 1383-1395.

Román-Cascón, C., C. Yagüe, M. Sastre, G. Maqueda, F. Salamanca, S. Viana, (2012), Observations and WRF simulations of fog events at the Spanish Northern Plateau, *Advances in Science and Research*, 8(1), 11-18.

Sanjay, J. (2008), Assessment of atmospheric boundary-layer processes represented in the numerical model MM5 for a clear sky day using LASPEX observations, *Boundary-layer meteorology*, 129(1), 159-177.

Shin, H. H., and S.-Y. Hong (2011), Intercomparison of planetary boundary-layer parametrizations in the WRF model for a single day from CASES-99, *Boundary-Layer Meteorology*, 139(2), 261-281.

Skamarock, W. C., J. B. Klemp, J. Dudhia, D. O. Gill, D. M. Barker, M. G. Duda, X.-Y. Huang, W. Wang, and J. G. Powers (2008), G.: A description of the Advanced Research WRF version 3, paper presented at NCAR Tech. Note NCAR/TN-475+ STR, Citeseer.

Smith, R. K., and G. L. Thomsen (2010), Dependence of tropical-cyclone intensification on the boundary-layer representation in a numerical model, *Quarterly Journal of the Royal Meteorological Society*, 136(652), 1671-1685.

Steele, C., S. Dorling, R. Von Glasow, J. Bacon, (2013), Idealized WRF model sensitivity simulations of sea breeze types and their effects on offshore windfields, *Atmospheric Chemistry and Physics*, 13(1), 443.

Su, L., and J. C. Fung (2015), Sensitivities of WRF-Chem to dust emission schemes and land surface properties in simulating dust cycles during springtime over East Asia, *Journal of Geophysical Research: Atmospheres*, 120(21), 11,215-211,230.

Sullivan, P. P., J. C. McWilliams, and C.-H. Moeng (1994), A subgrid-scale model for large-eddy simulation of planetary boundary-layer flows, *Boundary-Layer Meteorology*, 71(3), 247-276.

Wang, C. g., L. Feng, C. Le, Y. Jiade, and J. Hai-Mei (2017a), Comparison and analysis of several planetary boundary layer schemes in WRF model between clear and overcast days, *Chinese Journal of Geophysics*, 60(2), 141-153.

Wang, Y., S. Di Sabatino, A. Martilli, Y. Li, M. Wong, E. Gutiérrez, and P. Chan (2017b), Impact of land surface heterogeneity on urban heat island circulation and sea-land breeze circulation in Hong Kong, *Journal of Geophysical Research: Atmospheres*, 122(8), 4332-4352.

Wang, Z., A. Duan, and G. Wu (2014), Impacts of boundary layer parameterization schemes and air-sea coupling on WRF simulation of the East Asian summer monsoon, *Science China Earth Sciences*, 57(7), 1480-1493.

Xie, B., J. C. Fung, A. Chan, and A. Lau (2012), Evaluation of nonlocal and local planetary boundary layer schemes in the WRF model, *Journal of Geophysical Research: Atmospheres*, 117(D12).

Yerramilli, A., V. S. Challa, V. B. R. Dodla, H. P. Dasari, J. H. Young, C. Patrick, J. M. Baham, R. L. Hughes, M. G. Hardy, and S. J. Swanier (2010), Simulation of surface ozone pollution in the central gulf coast region using WRF/Chem Model: Sensitivity to PBL and Land Surface Physics, *Advances in Meteorology*, 2010.

Yver, C., H. Graven, D. D. Lucas, P. Cameron-Smith, R. Keeling, R. Weiss, (2013), Evaluating

598 transport in the WRF model along the California coast, *Atmospheric Chemistry & Physics*, 13(4).
599 Zhang, D.-L., and W.-Z. J. Zheng (2004), Diurnal cycles of surface winds and temperatures as
600 simulated by five boundary layer parameterizations, *Journal of Applied Meteorology and Climatology*,
601 43(1), 157-169.